Original Research

An Interpretable Multidimensional Acoustic Physiology Map for COPD Using Digital Lung Sounds

İhsan Topaloğlu, MD[1] Çağrı Atasoy, MD[1] Aylin Bayram, MD[1] Gülfem Özduygu, MD[2] Mutlu Onur Güçsav, MD[3] Damla Serçe Unat, MD[3] Soner Kına, MD[4] Yekta Bektaş, MD[4] Furkan Halifeoğlu, MD[4] Arif Metehan Yıldız, PhD[5]

[1] Department of Pulmonology, Faculty of Medicine, Kafkas University, Kars, Turkey

[2] Department of Pulmonology, Yedikule Chest Diseases and Thoracic Surgery Training and Research Hospital, University of Health Science, Istanbul, Turkey

[3] Department of Pulmonology, Çiğli Regional Training and Research Hospital, İzmir Bakırçay University, İzmir, Türkiye

[4] Department of Anesthesiology and Reanimation, Faculty of Medicine, Kafkas University, Kars, Türkiye

[5] Department of Computer Engineering, Faculty of Engineering, Ardahan University, Ardahan, Turkey

Address correspondence to:
İhsan Topaloğlu, MD
Department of Pulmonology
Faculty of Medicine
Kafkas University
Kars, Turkey
Phone: +90 530 122 63 11
Email: ras-topal@hotmail.com

Running Head: **Interpretable Acoustic Map for COPD**

Keywords: COPD; lung sound analysis; digital auscultation; acoustic indices; machine learning

Abbreviations**:** COPD, chronic obstructive pulmonary disease; MRF, median respiratory frequency; LTEI, long-term energy index; SubH, subharmonic index; HDI, harmonicity deviation index; PCA, principal component analysis; PERMANOVA, permutational multivariate analysis of variance; CORSA, Computerized Respiratory Sound Analysis; AI, artificial intelligence; GOLD, Global Initiative for Chronic Obstructive Lung Disease; STROBE, Strengthening the Reporting of Observational Studies in Epidemiology; CT, computed tomography; BMI, body mass index; FEV1, forced expiratory volume in 1 second; FVC, forced vital capacity; SD, standard deviation; IQR, interquartile range; STFT, short-time Fourier transform;

Published online June 1, 2026 https://doi.org/10.15326/jcopdf.2025.0746

Funding Support: None

Date of Acceptance: May 22, 2026 | ***Published Online Date***: June 1, 2026

Citation: Topaloğlu İ, Atasoy Ç, Bayram A, et al. An interpretable multidimensional acoustic physiology map for COPD using digital lung sounds. *Chronic Obstr Pulm Dis*. 2026; Published online June 1, 2026.
https://doi.org/10.15326/jcopdf.2025.0746

This article has an online supplement.

Abstract

Background: Lung sound analysis may capture chronic obstructive pulmonary disease (COPD) related physiology, but many methods are hard to interpret clinically. We developed a multidimensional acoustic physiology map using four indices from digital lung sounds: median respiratory frequency (MRF), long-term energy index (LTEI), subharmonic index (SubH), and harmonicity deviation index (HDI).

Methods: In this single-center retrospective study, 235 adults were classified as Healthy (n=62), Stable COPD (n=85), or COPD exacerbation (n=88). We analyzed 1,403 posterior thoracic 15-s recordings. Between-group differences in the four indices were tested with the Kruskal–Wallis test; when significant, Dunn post-hoc pairwise comparisons were performed with Holm adjustment. Multidimensional separation was evaluated in the z-scored four-index space using principal component analysis (PCA) and permutational multivariate analysis of variance. All tests were two-sided with P-value < 0.05 considered significant.

Results: Overall group differences were significant for MRF (P-value $=1.36\times10^{-5}$), SubH (P-value $=3.29\times10^{-6}$), and HDI (P-value $=4.74\times10^{-8}$), whereas LTEI did not show a statistically significant overall effect (P-value =0.086). Post-hoc analyses indicated that MRF and SubH primarily separated Stable COPD from both Healthy and COPD exacerbation, while HDI primarily separated COPD exacerbation from Healthy and Stable COPD. Group distributions were visualized with triangular heatmaps and summarized in a three-axis model.

Conclusions: Complementary acoustic indices reflect distinct domains of COPD-related sound generation and transmission. Although standalone classification performance was limited, the proposed map provides an interpretable framework for digital auscultation phenotyping and future composite scoring.

Published online June 1, 2026 https://doi.org/10.15326/jcopdf.2025.0746

INTRODUCTION

Chronic obstructive pulmonary disease (COPD) is a heterogeneous disorder with stable periods and acute exacerbations. Exacerbations are characterized by rapid worsening of dyspnea, cough, and/or sputum and drive treatment intensity, hospitalization, and follow-up [1].

Although lung sounds constitute a fundamental component of bedside respiratory assessment, conventional auscultation remains largely subjective. The increasing use of digital stethoscopes and computer-assisted analysis techniques has enabled the quantification of respiratory sounds across time–frequency–energy domains, allowing for more reproducible and standardized measurements; guidelines such as those from Computerized Respiratory Sound Analysis (CORSA) have further supported terminology and measurement standardization in this field [2,3]. Systematic reviews have demonstrated that computerized lung sound analysis holds clinically meaningful potential for detecting abnormal respiratory sounds [4]. Despite rapid advances in AI (Artificial İnteligence) and machine learning, many studies emphasize classification over pathophysiological interpretability [5–7].

In COPD, airflow limitation, energy instability, heterogeneous small-airway narrowing, and nonlinear vibration may be encoded in the spectral and temporal structure of respiratory sounds [6]. Therefore, rather than relying on a single metric, the combined evaluation of complementary indices may enhance both discriminatory performance and pathophysiological interpretability.

In this study, we proposed four recording-level indices derived from digital lung sound recordings—Median Respiratory Frequency (MRF), Long-Term Energy Index (LTEI), Subharmonic Index (SubH), and Harmonicity Deviation Index (HDI)—to jointly describe frequency distribution, temporal energy instability, nonlinear/subharmonic structure, and spectral organization, respectively.

MATERIALS AND METHODS

Study Design and Ethical Approval

Published online June 1, 2026 https://doi.org/10.15326/jcopdf.2025.0746

This single-center, cross-sectional retrospective study was conducted at the Chest Diseases Clinic of Kafkas University Faculty of Medicine Hospital. We reviewed electronic medical records and digitally archived lung sound recordings obtained during routine care between June 1, 2023 and November 30, 2025, and reported the study in accordance with STROBE.

Data were analyzed in anonymized form. The protocol complied with the Declaration of Helsinki and was approved by the Kafkas University Clinical Research Ethics Committee (KAÜ-80576354-050-099/813; December 2, 2025). The Ethics Committee explicitly waived the requirement for written informed consent, determining that the study met the criteria for waiver: the design was retrospective, all personal identifiers were removed prior to analysis, and the recordings had been obtained exclusively as part of routine clinical care with no study-specific procedures performed.

Adults (≥18 years) were eligible if lung sound recordings were obtained with the routine protocol and corresponding clinical and spirometric data were available. We excluded recordings with insufficient duration, extensive artifacts, or missing audio files; concurrent major pleural pathology or acute cardiovascular events at recording; and incomplete clinical or spirometric data.

Participants and Clinical Groups

We included 235 participants and categorized them as Healthy, Stable COPD, or COPD Exacerbation according to clinical status at the time of recording.

Demographics, smoking history (pack-years), comorbidities, clinical findings, spirometry, and CT-reported emphysema status corresponding to the recording date were extracted from the hospital information system. COPD diagnosis was confirmed using GOLD 2024 criteria [8].

Healthy participants were identified from archived recordings of individuals who had undergone routine occupational health surveillance at our institution. As these individuals attended for occupational screening rather than respiratory complaints, they represented a population free of known respiratory disease at the time of recording, providing an appropriate reference group for acoustic comparison. Eligible healthy participants were

Published online June 1, 2026 https://doi.org/10.15326/jcopdf.2025.0746

required to have no chronic respiratory symptoms, no known chronic lung disease, no evidence of acute lower respiratory tract infection or pneumonia at the time of recording, and normal spirometry. Chest auscultation was performed by a pulmonologist; the absence of pathological lung sounds was defined as the absence of wheeze, crackles, rhonchi, stridor, or focal/asymmetric reduction in breath sounds. Normal spirometry was defined as post-bronchodilator FEV_1 and FVC ≥80% predicted and FEV_1/FVC ≥0.70 [9,10]. Smokers without clinical or spirometric COPD were eligible only if all of these criteria were satisfied.

Stable COPD patients had post-bronchodilator FEV_1/FVC <0.70 and were clinically stable at recording, defined as no exacerbation, systemic corticosteroid/antibiotic use, or change in maintenance inhaler therapy within ≥4 weeks, with stable vital signs documented in physician notes.

COPD exacerbation was defined per GOLD 2024 and required recordings obtained during the exacerbation period. Exacerbation was an acute worsening of dyspnea and/or cough and sputum compared with stable state, requiring additional treatment and typically lasting <14 days [1]. Patients on invasive mechanical ventilation were excluded; technically adequate recordings under noninvasive ventilation or oxygen therapy were included.

Digitally archived posterior thoracic recordings were screened and three datasets were defined (370 recordings/62 individuals; 508/85; 525/88). Each 15-s recording was analyzed as a region-specific observation.

In COPD, emphysema status was determined qualitatively (present/absent) from routine chest CT reports: cases explicitly reporting emphysema were included, whereas reports stating absent emphysema or not mentioning emphysema were excluded. To provide an objective CT-based assessment of emphysema, available chest CT scans were analyzed using automated lung segmentation with two deep learning–based tools (TotalSegmentator and LungMask). After segmentation of the lung parenchyma, emphysema burden was quantified as the percentage of low-attenuation area below −950 Hounsfield units (LAA–950). LAA–950 was calculated separately for each segmentation model, and the mean of the two measurements was used as the final emphysema value in the analysis. Image

Published online June 1, 2026 https://doi.org/10.15326/jcopdf.2025.0746

analysis was performed blinded to clinical group assignment. This approach ensured that the study population reflected a radiologically confirmed emphysematous COPD subgroup.

To address the possibility of selection bias related to exclusions, the available baseline characteristics of excluded screened cases were also summarized and reviewed descriptively in relation to the final analytic cohort. Because several exclusions were related to incomplete clinical or spirometric data, the excluded cases were not treated as a formal comparison group in the primary analyses.

Lung Sound Recording Protocol

Lung sound recordings were obtained under standardized conditions using a Littmann CORE digital stethoscope (3M, St. Paul, MN, USA); all participants were seated and instructed to breathe deeply and rhythmically through the mouth. Recordings were performed in a quiet outpatient examination room or, for hospitalized patients, in a single-occupancy inpatient room with the door closed to minimize ambient noise; a seated position was maintained in both settings. Patients with COPD exacerbation who were receiving intermittent noninvasive ventilation (NIV) were recorded during a period when NIV was not in use; no recordings were obtained while NIV was actively applied. Auscultation was performed at six posterior thoracic sites (bilaterally at the interscapular, mid-scapular, and infrascapular levels). A 15-second recording was obtained from each site, yielding a total of 90 seconds of lung sound data per participant. All recordings were digitally stored with a sampling frequency of 44.1 kHz and 16-bit resolution.

Segments containing prominent artifacts due to speech, coughing, patient or stethoscope movement, or cable contact were identified through combined visual and auditory inspection of waveforms, spectra, and spectrograms and were excluded. If artifacts affected the majority of a 15-second segment, the entire segment was discarded. Only recordings of sufficient technical quality were included in the statistical analyses. Because each 15-

Published online June 1, 2026 https://doi.org/10.15326/jcopdf.2025.0746

second recording contained multiple respiratory cycles, inspiratory and expiratory phases were not manually separated; all acoustic analyses were conducted at the recording level, and the calculated acoustic indices (MRF, LTEI, SubH, and HDI) were expressed as single representative values for each segment.

Signal Preprocessing and Time–Frequency Analysis

Raw lung sound recordings were first processed using a 100–1600 Hz band-pass filter to attenuate low-frequency chest wall noise and high-frequency interference. Subsequently, amplitude normalization was applied to reduce inter-recording amplitude variability, and potential DC offsets were corrected to center the signal around zero.

Each 15-second recording was segmented into overlapping windows of 200 ms duration with 50% overlap for short-time analysis. For each window, the short-time Fourier transform (STFT) was computed, and the power spectrum was obtained as:

.

These power spectra served as the primary data source for the calculation of all acoustic markers.

Calculation of Acoustic Parameters

To quantitatively reflect different aspects of airway physiology, four acoustic markers were defined: Median Respiratory Frequency (MRF), Long-Term Energy Index (LTEI), Subharmonic Index (SubH), and Harmonicity Deviation Index (HDI). All markers were calculated as median-based summaries of spectral and energy measures derived from short-time frames.

Median Respiratory Frequency (MRF) represents the dominant frequency of lung sounds and reflects turbulence related to airway narrowing. For each frame, the power spectrum within the 100–1600 Hz range was examined, and the frequency at which the maximum spectral power occurred was defined as the dominant frequency:

Published online June 1, 2026 https://doi.org/10.15326/jcopdf.2025.0746

For a given 15-second recording, the median of all frame-level dominant frequencies was recorded as the MRF.

Long-Term Energy Index (LTEI) is an energy-based index reflecting the long-term stability of the respiratory sound signal. Instantaneous energy was calculated for each 200 ms frame. The mean energy μE and standard deviation σE across all frames were then computed, and LTEI was defined as the ratio σE/μE.

Across all frames, the mean energy μ_E and standard deviation σ_E were calculated, and LTEI was defined as the ratio σ_E/μ_E.

This ratio represents the relative degree of temporal energy fluctuation and yields a single LTEI value for each recording.

Subharmonic Index (SubH) quantifies the relative contribution of subharmonic components in lung sounds. For each frame, after identifying the dominant frequency , three narrow frequency bands (±20 Hz) centered at , and were defined. The sum of spectral power within these bands was calculated as subharmonic energy. The total spectral power within the 100–1600 Hz band was defined as EtotalE_{\text{total}}Etotal. The frame-level subharmonic ratio was computed as the ratio of subharmonic energy to total energy. For each 15-second recording, the median of all frame-level SubH values was used as the recording-level SubH.

Within the same frame, the total power of all spectral components in the 100–1600 Hz band was defined as :

The frame-level subharmonic ratio was calculated as:

Published online June 1, 2026 https://doi.org/10.15326/jcopdf.2025.0746

For each 15-second recording, the median of all frame-level SubHi_ii values was used as the SubH value of the corresponding recording:

The Harmonicity Deviation Index (HDI) was defined to quantify spectral irregularity in the harmonic structure. For each frame, the power spectrum was evaluated based on the differences between adjacent frequency bins:

where M denotes the number of frequency bins. In signals with a regular harmonic structure, HDI is expected to be lower, whereas higher values are anticipated in patterns with increased noise and structural distortion. For each recording, the median of all frame-level values was defined as the HDI value of that recording:

Thus, MRF, LTEI, SubH, and HDI were used as four complementary acoustic markers summarizing each 15-second lung sound recording in the time–frequency domain.

Statistical Analysis

Continuous variables are presented as mean ± standard deviation (SD) or as median (interquartile range, IQR), as appropriate. Categorical variables are presented as counts and percentages. Between-group comparisons (Healthy, Stable COPD, COPD exacerbation) used the chi-square test for categorical variables. For continuous variables, one-way ANOVA was used when applicable; otherwise, the Kruskal–Wallis test was used. Acoustic analyses were performed on 15-s recording segments. The primary acoustic indices were MRF, LTEI, SubH, and HDI. Overall group differences for these indices were tested using the Kruskal–Wallis test. Pairwise post-hoc comparisons were performed using Dunn's test with Holm adjustment. For multivariate analyses, the four indices were z-standardized and

Published online June 1, 2026 https://doi.org/10.15326/jcopdf.2025.0746

projected using principal component analysis (PCA). Group separation in the standardized four-index space was tested using permutational multivariate analysis of variance (PERMANOVA) with Euclidean distance and permutation-basedP-value values. All tests were two-sided, and P-value < 0.05 was considered statistically significant.

RESULTS

A total of 322 archived cases were screened, of which 87 were excluded according to the predefined criteria, leaving 235 participants in the final analytic cohort: 62 healthy individuals, 85 patients with stable COPD, and 88 patients with COPD exacerbation (Supplementary Figure S1). After recording-level quality control, the acoustic dataset comprised 1,403 posterior thoracic recordings of 15 seconds' duration, including 370 recordings from healthy individuals, 508 from patients with stable COPD, and 525 from patients with COPD exacerbation. Baseline characteristics of the analytic cohort are presented in Table 1.

Quantitative emphysema burden (LAA–950) was significantly higher in the COPD exacerbation group than in the stable COPD group (median 27.61% [IQR 14.18–35.39] vs. 15.27% [IQR 4.81–32.99], P-value = 0.002). Detailed quantitative emphysema data are presented in Supplementary Table 1.

Between-group differences for the four prespecified indices (MRF, LTEI, SubH, and HDI) were assessed using the Kruskal–Wallis test, followed by Dunn's post-hoc tests with Holm adjustment for multiple comparisons.

These median patterns are visualized in Figure 1.

MRF.

Overall group differences were significant (Kruskal–Wallis p=1.36e-05). MRF was lower in Stable COPD than in Healthy (P-value =3.29e-05) and COPD exacerbation (P-value =0.0007), while Healthy and COPD exacerbation did not differ (P-value =0.2561).

Published online June 1, 2026 https://doi.org/10.15326/jcopdf.2025.0746

SubH.

A pronounced overall difference was observed (Kruskal–Wallis p=3.29e-06). SubH was higher in Stable COPD than in Healthy (P-value =0.0001) and COPD exacerbation (P-value =1.74e-05), whereas Healthy and COPD exacerbation were similar (P-value =0.9121).

HDI.

HDI showed the strongest overall separation (Kruskal–Wallis p=4.74e-08). HDI was higher in COPD exacerbation than in Healthy (P-value =1.15e-06) and Stable COPD (P-value =3.09e-06), while Healthy and Stable COPD did not differ (P-value =0.5048).

LTEI.

LTEI did not show a statistically significant overall difference across groups (Kruskal–Wallis p=0.0858), and no pairwise comparison remained significant after Holm correction (Table 3).

Multidimensional separation using the four-index acoustic map.

To test whether the four indices jointly capture a multivariate shift across clinical states, we applied a permutation-based multivariate analysis of variance (PERMANOVA; Euclidean distance on z-scored indices). Overall group separation was significant (pseudo-$F=5.19$, $R^2=0.0074$, permutation p=0.0001; 9,999 permutations).

A two-dimensional PCA projection of the z-scored four-index space showed partially overlapping clusters with modest centroid shifts across clinical groups (Figure S1), consistent with the small but significant multivariate separation observed by PERMANOVA (Table 4).

A schematic summary of the multidimensional acoustic physiology map is shown in Figure 2.

DISCUSSION

Published online June 1, 2026 https://doi.org/10.15326/jcopdf.2025.0746

Although lung sounds remain one of the fundamental tools in the clinical assessment of patients with COPD, quantitative analysis of respiratory sounds is a relatively underexplored field, and most existing studies have focused on isolated markers such as the presence of wheezes or crackles, dominant frequency, or a limited number of spectral features [4,8]. In contrast, the present study aimed to evaluate airway physiology within a multidimensional acoustic framework by using four composite acoustic indices (MRF, LTEI, SubH, and HDI) derived from digital lung sound recordings obtained from healthy individuals, patients with stable COPD, and patients during COPD exacerbation.

It is well established that respiratory sounds originate from turbulent airflow within the airways and that their frequency content is determined by airway caliber, airflow velocity, and the transmission properties of the lung parenchyma and chest wall [3,11]. Normal lung tissue behaves as a low-pass filter, attenuating higher-frequency components while transmitting lower frequencies more efficiently. Alterations in parenchymal structure, fluid content, or consolidation may modify this filtering effect [12]. Flow-standardized studies have shown that median frequency tends to increase in asthma compared with healthy controls, whereas in COPD it may be similar to or lower than in controls, potentially reflecting changes in parenchymal structure and sound transmission [13].

In our results, MRF differed among healthy individuals, patients with stable COPD, and those with COPD exacerbation, with the lowest median values observed in the stable COPD group, while the healthy and COPD exacerbation groups exhibited relatively similar median levels (Table 2-Table 3). This pattern is consistent with a pathophysiological framework in which chronic airway narrowing accompanied by hyperinflation and parenchymal destruction attenuates higher-frequency components generated in central airways, thereby shifting the chest wall–recorded spectrum toward lower frequencies [3,12,13]. During exacerbations, increased turbulence and wheeze episodes in narrowed segments may tend to elevate dominant frequencies, whereas coarse rhonchi, prolonged expiration, secretion retention, and reflex limitation of inspiratory flow may counterbalance this effect. Moreover, the use of median-based recording-level MRF likely limits the influence of brief high-frequency events [3,4]. Together, these opposing forces may account for the absence of a significant difference between Healthy and COPD

Published online June 1, 2026 https://doi.org/10.15326/jcopdf.2025.0746

exacerbation groups: rather than reflecting physiological equivalence, their convergent MRF values likely arise from distinct mechanisms — chronic low-frequency shift in one direction and acute turbulence-driven elevation in the other — that net to a similar recording-level median.

LTEI reflects the temporal stability of respiratory sound energy — a property mechanistically linked to the near-quadratic relationship between instantaneous airflow and recorded sound power [14,15], such that LTEI can be interpreted as a surrogate for the temporal variability of the airflow–acoustic power transfer function.

In our dataset, LTEI values were numerically higher in the healthy group than in both COPD groups, while stable COPD and COPD exacerbation groups exhibited similar and relatively lower LTEI values (Table 2-Table 3). However, the overall group effect did not reach statistical significance (P-value = 0.086), and no pairwise comparison remained significant after multiplicity correction; therefore, this pattern should be interpreted as exploratory. This directionality is compatible with the well-established presence of tidal expiratory flow limitation, chronic hyperinflation, and dynamic airway compression in COPD, which may constrain airflow around a plateau despite increased respiratory effort [8, 16, 17]. Furthermore, physiological studies of lung sound generation and transmission have shown that lung volume, regional ventilation distribution, and parenchymal properties strongly modulate the temporal and spatial characteristics of chest wall–recorded sounds [18, 19]. In heterogeneous small airway disease and emphysema, respiratory sound generation may arise from multiple asynchronous micro-turbulence sources rather than a few dominant bronchial jets; the statistical averaging of these sources, together with the viscoelastic damping properties of emphysematous parenchyma, could result in a flatter, less fluctuating temporal energy profile. Consequently, the observation of lower and similar LTEI values in both stable COPD and COPD exacerbation groups may reflect a "locking" of acoustic output within a narrowed energy band due to chronic airway and parenchymal damage, further reinforced by effort limitation. As this constraining mechanism operates similarly across both COPD states, the resulting narrowing of the acoustic dynamic range may reduce rather than amplify between-group differences, which

Published online June 1, 2026 https://doi.org/10.15326/jcopdf.2025.0746

may account for the absence of statistical significance despite the numerically observed trend.

Unlike binary wheeze detection, SubH quantifies coherent subharmonic energy arising from airway wall vibration and nonlinear dynamics in narrowed small airways. Prior studies using wavelet-based and bicoherence analyses have demonstrated that wheezes represent harmonically and subharmonically rich structures rather than simple single-frequency tones [6]. More recent deep learning–based lung sound studies have also shown that nonlinear and harmonic features of adventitious sounds, particularly wheezes, contribute meaningfully to classification performance [20,21].

In the present study, median SubH values were highest in the stable COPD group, while healthy individuals and patients during COPD exacerbation exhibited similar and lower values (Table 2-Table 3). This pattern suggests that SubH does not increase monotonically with clinical severity. Instead, it appears to reflect persistent nonlinear subharmonic patterns associated with chronic small airway remodeling. In stable COPD, heterogeneous luminal narrowing and segmental differences in elasticity may provide favorable conditions for repetitive and relatively stable airway wall flutter, leading to energy accumulation in subharmonic bands. During exacerbations, although the underlying structural substrate persists, edema, increased secretions, and abrupt airway closure–reopening events may disrupt the coherence of these oscillations, rendering subharmonic energy more episodic and temporally dispersed. As a result, the median SubH calculated over 15-second recordings may not increase relative to the stable state. This mechanism may also clarify the apparent convergence between Healthy and COPD exacerbation groups: while healthy individuals likely exhibit low SubH due to the absence of the structural substrate required for coherent subharmonic generation, exacerbation patients may show similarly low values despite persistent small airway remodeling, as acute disruption of oscillatory coherence may limit the consistent accumulation of subharmonic energy at the recording level. The similar SubH values in these two groups may therefore reflect mechanistically distinct states rather than comparable airway physiology.

In normal lungs, particularly during inspiration, respiratory sounds tend to exhibit

Published online June 1, 2026 https://doi.org/10.15326/jcopdf.2025.0746

smoother spectral profiles, reflecting relatively laminar or pre-turbulent airflow in larger airways and homogeneous parenchymal [18,22]. In contrast, in COPD, small airway narrowing, luminal irregularity, wall thickening, secretion accumulation, and heterogeneous time constants generate multiscale turbulence and flow separation throughout the bronchial tree, resulting in fragmented, "sawtooth-like" spectral patterns [17,18]. HDI thus represents a distinct acoustic dimension capturing the degree of spectral organization versus chaotic fragmentation [25].

Consistent with this framework, median HDI values were lowest in the healthy group and modestly higher in both stable COPD and COPD exacerbation groups (Table 2-Table 3). In healthy individuals, smoother airway geometry and homogeneous parenchyma preserve spectral continuity at the chest wall, yielding lower HDI values [18,22]. In COPD, patchy airway narrowing, mucosal irregularity, mucus plugs, and emphysema-related elastic heterogeneity generate numerous small turbulence foci that disrupt spectral continuity and increase HDI [23,24]. The lack of a marked difference in HDI between stable COPD and exacerbation groups suggests that HDI is primarily sensitive to chronic structural remodeling and persistent airway geometric irregularity, with acute exacerbation-related processes exerting a comparatively limited additional effect.

The observed separation in MRF, SubH, and HDI alongside the non-significant overall behavior of LTEI (Tables 2–4) supports the view that COPD-related acoustic change is distributed across distinct, complementary domains of sound generation and transmission. Together, these four domains — frequency shift, energy stability, subharmonic activity, and spectral disorganization — constitute complementary acoustic dimensions of COPD-related airway physiology. The triangular heatmaps (Figure 1) provide a compact, region-resolved view of how these domains vary across clinical states, whereas the three-axis acoustic physiology model (Figure 2) integrates the indices into an interpretable structure that links each metric to its dominant mechanistic axis. Together, these elements define an acoustic physiology map that organizes complementary information across mechanisms, rather than compressing COPD lung sounds into a single unidimensional summary.

Published online June 1, 2026 https://doi.org/10.15326/jcopdf.2025.0746

Beyond univariate comparisons, PERMANOVA in the z-scored four-index space indicated a statistically significant but small multivariate separation among clinical states (Table 4; Figure S1). Pairwise results suggested that Stable COPD was the most consistently separated state, whereas separation between Healthy and COPD exacerbation was limited. The low R^2 values are consistent with the primary aim of this work: rather than classifying clinical states, the four indices were designed to characterize the acoustic-physiological mechanisms that underlie each clinical state — a dimension not captured by standard assessment. In this sense, the proposed map complements rather than replaces existing diagnostic tools, with potential relevance for disease monitoring, phenotyping, and the development of mechanistically interpretable digital biomarkers.

Limitations of the Study

Lung sound recordings were obtained without simultaneous airflow or volume measurements (e.g., pneumotachography); consequently, inter-individual differences in respiratory rate, tidal volume, and inspiratory flow — all known to influence lung sound frequency content and amplitude — could not be controlled for. This constraint is particularly relevant for MRF, whose dominant frequency is sensitive to airflow velocity, and for LTEI, which captures energy fluctuations in respiratory sounds that are inherently linked to instantaneous airflow variability. Some exacerbation recordings were acquired under oxygen therapy or noninvasive ventilation, which may also have affected acoustic characteristics. Because only COPD cases with radiologically reported emphysema were included, findings may not generalize to non-emphysematous phenotypes. Analyses were conducted primarily at the recording level; multiple recordings per participant may have affected independence assumptions, and future studies should incorporate patient-level validation or models accounting for repeated measures and potential confounders (e.g., age and BMI). As a single-center study, external validity remains to be established; multicenter validation across diverse COPD phenotypes and clinical settings is warranted. In addition, although a substantial number of screened cases were excluded, the reasons for exclusion were predefined and are now reported transparently, which reduces but does not eliminate the possibility of selection bias.

Published online June 1, 2026 https://doi.org/10.15326/jcopdf.2025.0746

Declaration of Interest

The authors declare no competing interests.

Data availability

The data supporting the findings are available within the article; de-identified data may be provided by the corresponding author upon reasonable request.

Author contributions:

I.T. and C.A.: study design. I.T., C.A., A.B.: data collection and data cleaning. G.O., M.O.G.: clinical review and manuscript review. Y.B., A.M.Y.: signal processing and software. D.S.U., S.K., F.H.: analysis support. All authors: writing and final approval.

Consent for publication

Not applicable (no identifiable participant information); all authors approved the final manuscript.

Published online June 1, 2026 https://doi.org/10.15326/jcopdf.2025.0746

References

1. Global Initiative for Chronic Obstructive Lung Disease (GOLD). Pocket guide to COPD diagnosis, management, and prevention: a guide for health care professionals. 2025 report. Version 1.2. Published December 13, 2024. Accessed December 24, 2025. https://goldcopd.org/wp-content/uploads/2024/12/Pocket-Guide-2025-v1.2-FINAL-covered-13Dec2024_WMV.pdf.

2. Sovijärvi ARA, Dalmasso F, Vanderschoot J, Malmberg LP, Righini G, Stoneman SAT. Definition of terms for applications of respiratory sounds. Eur Respir Rev. 2000;10(77):597-610.

3. Reichert S, Gass R, Brandt C, Andrès E. Analysis of respiratory sounds: state of the art. Clin Med Circ Respirat Pulm Med. 2008;2:45-58. doi:10.4137/CCRPM.S530.

4. Gurung A, Scrafford CG, Tielsch JM, et al. Computerized lung sound analysis as a diagnostic aid for the detection of abnormal lung sounds: a systematic review and meta-analysis. Respir Med. 2011;105(9):1396-1403. doi:10.1016/j.rmed.2011.05.007.

5. Huang DM, Huang J, Qiao K, et al. Deep learning-based lung sound analysis for intelligent stethoscope. Mil Med Res. 2023;10(1):44. doi:10.1186/s40779-023-00479-3.

6. Taplidou SA, Hadjileontiadis LJ. Nonlinear analysis of wheezes using wavelet bicoherence. Comput Biol Med. 2007;37(4):563-570. doi:10.1016/j.compbiomed.2006.11.007.

7. Xu X, Sankar R. Classification and recognition of lung sounds using artificial intelligence and deep learning: a literature review. Big Data Cogn Comput. 2024;8(10):127. doi:10.3390/bdcc8100127.

8. Global Initiative for Chronic Obstructive Lung Disease (GOLD). Pocket guide to COPD diagnosis, management, and prevention: a guide for health care professionals. 2024 report. Version 1.2. Updated January 11, 2024. Accessed December 24, 2025. https://goldcopd.org/wp-content/uploads/2024/02/POCKET-GUIDE-GOLD-2024-ver-1.2-11Jan2024_WMV.pdf.

Published online June 1, 2026 https://doi.org/10.15326/jcopdf.2025.0746

9. Stanojevic S, Kaminsky DA, Miller MR, et al. ERS/ATS technical standard on interpretive strategies for routine lung function tests. Eur Respir J. 2022;60(1):2101499. doi:10.1183/13993003.01499-2021.

10. Graham BL, Steenbruggen I, Miller MR, et al. Standardization of spirometry 2019 update: an official American Thoracic Society and European Respiratory Society technical statement. Am J Respir Crit Care Med. 2019;200(8):e70-e88. doi:10.1164/rccm.201908-1590ST.

11. Pasterkamp H, Brand PLP, Everard M, Garcia-Marcos L, Melbye H, Priftis KN. Towards the standardisation of lung sound nomenclature. Eur Respir J. 2016;47(3):724-732. doi:10.1183/13993003.01132-2015.

12. Zimmerman B, Williams D. Lung sounds. In: StatPearls [Internet]. Treasure Island (FL): StatPearls Publishing; 2025 Jan-. Updated August 28, 2023. Accessed December 24, 2025. https://www.ncbi.nlm.nih.gov/books/NBK537253/.

13. Malmberg LP, Pesu L, Sovijärvi AR. Significant differences in flow standardised breath sound spectra in patients with chronic obstructive pulmonary disease, stable asthma, and healthy lungs. Thorax. 1995;50(12):1285-1291. doi:10.1136/thx.50.12.1285.

14. Kraman SS. The relationship between airflow and lung sound amplitude in normal subjects. Chest. 1984;86(2):225-229. doi:10.1378/chest.86.2.225.

15. Beck R, Rosenhouse G, Mahagnah M, Chow RM, Cugell DW, Gavriely N. Measurements and theory of normal tracheal breath sounds. Ann Biomed Eng. 2005;33(10):1344-1351. doi:10.1007/s10439-005-5564-7.

16. Tantucci C. Expiratory flow limitation: definition, mechanisms, methods, and significance. Pulm Med. 2013;2013:749860. doi:10.1155/2013/749860.

17. O'Donnell DE, Webb KA, Neder JA. Lung hyperinflation in COPD: applying physiology to clinical practice. COPD Res Pract. 2015;1:4. doi:10.1186/s40749-015-0008-8.

18. Pasterkamp H, Kraman SS, Wodicka GR. Respiratory sounds: advances beyond the stethoscope. Am J Respir Crit Care Med. 1997;156(3 Pt 1):974-987. doi:10.1164/ajrccm.156.3.9701115.

Published online June 1, 2026 https://doi.org/10.15326/jcopdf.2025.0746

19. Kiyokawa H, Pasterkamp H. Volume-dependent variations of regional lung sound amplitude and phase. J Appl Physiol (1985). 2002;93(3):1030-1038. doi:10.1152/japplphysiol.00110.2002.

20. Kim Y, Hyon Y, Jung SS, et al. Respiratory sound classification for crackles, wheezes, and rhonchi in the clinical field using deep learning. Sci Rep. 2021;11:17186. doi:10.1038/s41598-021-96724-7.

21. Dubey R, Bodade RM, Dubey D. Efficient classification of the adventitious sounds of the lung through a combination of SVM-LSTM-Bayesian optimization algorithm with features based on wavelet bi-phase and bi-spectrum. Res Biomed Eng. 2023;39:349-363. doi:10.1007/s42600-023-00270-2.

22. Malinina EV, Kulakov YV, Safronova MA, Tagiltsev AA, Kostin AE. Characteristics of flow-standardized inspiratory lung sounds in healthy subjects. Hum Physiol. 2014;40(4):440-449. doi:10.1134/S0362119714040112.

23. Copot D, De Keyser R, Derom E, Ionescu CM. Structural changes in the COPD lung and related heterogeneity. PLoS One. 2017;12(5):e0177969. doi:10.1371/journal.pone.0177969.

24. Stockley JA, Cooper BG, Stockley RA, Sapey E. Small airways disease: time for a revisit? Int J Chron Obstruct Pulmon Dis. 2017;12:2343-2353. doi:10.2147/COPD.S138540.

25. Ram A, Gupta B, Chaurasia A, Kumari A, Kumar R. Approaches for respiratory sound analysis in identification of respiratory diseases. Front Biomed Technol. 2024;11(2):286-295. doi:10.22034/fbt.2024.39318.

Published online June 1, 2026 https://doi.org/10.15326/jcopdf.2025.0746

Table 1. Baseline characteristics and recording counts of the analytic cohort by clinical group.

Variable	Healthy group (n=62)	Stable COPD (n=85)	COPD exacerbation (n=88)	p
Age, years	58.9 ± 11.3	65.2 ± 9.0	64.4 ± 9.3	0.000252
Sex, Male sex, n (%)	46 (74.2%)	73 (85.9%)	69 (78.4%)	0.194
BMI, kg/m²	22.7 ± 2.0	21.6 ± 2.4	21.4 ± 2.0	0.001470
FEV1/FVC, %	82.7 ± 3.2	59.7 ± 7.2	58.8 ± 7.4	<0.001
Number of recordings (15-s segments), n	370	508	525	—

Note: Data are shown as mean ± SD for continuous variables and as n (%) for categorical variables. Between-group comparisons: one-way ANOVA for continuous variables and chi-square test for sex. BMI, body mass index; COPD, chronic obstructive pulmonary disease; FEV1, forced expiratory volume in 1 second; FVC, forced vital capacity; SD, standard deviation. Dash (—) denotes not applicable.

Published online June 1, 2026 https://doi.org/10.15326/jcopdf.2025.0746

Table 2. Group-level distribution of primary acoustic indices (median [IQR]).

Index	Healthy	Stable COPD	COPD exacerbation	Kruskal–Wallis p
MRF	131.836 [123.047–145.508]	126.953 [119.141–139.648]	129.883 [121.094–148.438]	1.36e-05
LTEI	2.927 [1.787–4.605]	2.577 [1.709–4.112]	2.602 [1.790–4.001]	0.0858
SubH	0.093 [0.052–0.152]	0.123 [0.064–0.215]	0.096 [0.053–0.152]	3.29e-06
HDI	2.18e-05 [8.01e-06–5.83e-05]	2.10e-05 [8.19e-06–7.92e-05]	3.63e-05 [1.30e-05–1.39e-04]	4.74e-08

Note: Values are presented as median [interquartile range]. Overall between-group differences were assessed using the Kruskal–Wallis test. MRF: Median Respiratory Frequency; LTEI: Long-Term Energy Index; SubH: Subharmonic Index; HDI: Harmonicity Deviation Index; COPD: Chronic Obstructive Pulmonary Disease. IQR: Interquartile Range.

Published online June 1, 2026 https://doi.org/10.15326/jcopdf.2025.0746

Table 3. Pairwise post-hoc comparisons of acoustic indices between clinical groups.

Index	Healthy vs Stable COPD (P-value)	Healthy vs COPD exacerbation (P-value)	Stable COPD vs COPD exacerbation (P-value)
MRF	3.29e-05	0.2561	0.0007
LTEI	0.0959	0.1768	0.6191
SubH	0.0001	0.9121	1.74e-05
HDI	0.5048	1.15e-06	3.09e-06

Note: Pairwise comparisons were performed using Dunn's test with Holm adjustment for multiple comparisons. Adjusted P-values (P_adj) are reported. MRF: Median Respiratory Frequency; LTEI: Long-Term Energy Index; SubH: Subharmonic Index; HDI: Harmonicity Deviation Index; COPD: Chronic Obstructive Pulmonary Disease.

Published online June 1, 2026 https://doi.org/10.15326/jcopdf.2025.0746

Table 4. Pairwise multivariate group separation.

Comparison	n	Pseudo-F	R^2	p (perm)	P-value (Holm)
Healthy vs Stable COPD	878	7.88	0.0089	0.0001	0.0003
Healthy vs COPD exacerbation	895	2.31	0.0026	0.0429	0.0429
Stable COPD vs COPD exacerbation	1033	5.88	0.0057	0.0002	0.0004

Note: Group separation was assessed using permutational multivariate analysis of variance (PERMANOVA) with Euclidean distance on z-scored indices (9,999 permutations). Pseudo-F and R^2 values reflect effect size; permutation-based P-values are reported. MRF: Median Respiratory Frequency; LTEI: Long-Term Energy Index; SubH: Subharmonic Index; HDI: Harmonicity Deviation Index; COPD: Chronic Obstructive Pulmonary Disease.

Published online June 1, 2026 https://doi.org/10.15326/jcopdf.2025.0746

Figure 1. Triangular heatmaps of group medians for the four primary indices.

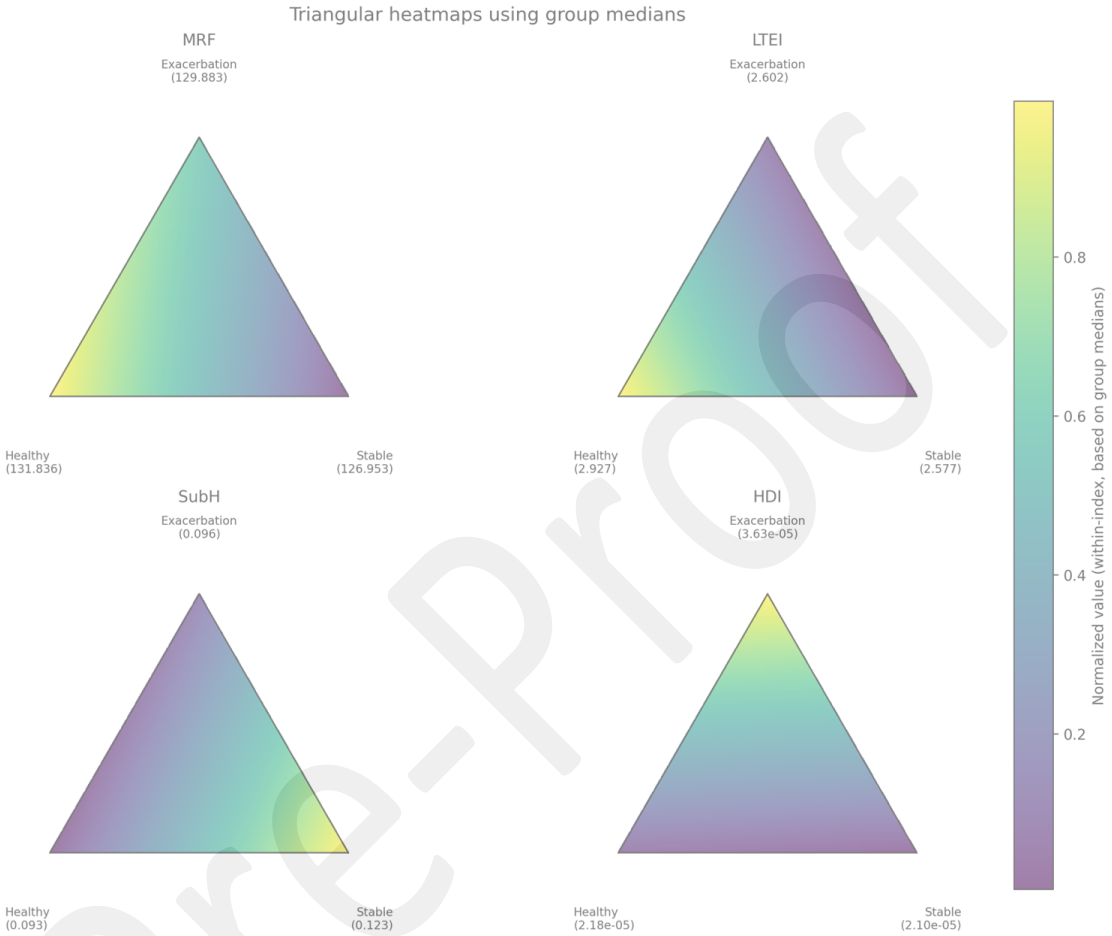

Note: Each triangle represents one index (MRF, LTEI, SubH, HDI). Vertex values in parentheses denote group medians (Healthy, Stable COPD, COPD exacerbation). Color indicates within-index normalization (0–1) based on the three group medians. MRF: Median Respiratory Frequency; LTEI: Long-Term Energy Index; SubH: Subharmonic Index; HDI: Harmonicity Deviation Index; COPD: Chronic Obstructive Pulmonary Disease.

Published online June 1, 2026 https://doi.org/10.15326/jcopdf.2025.0746

Figure 2. Conceptual multidimensional acoustic physiology map derived from group-level patterns.

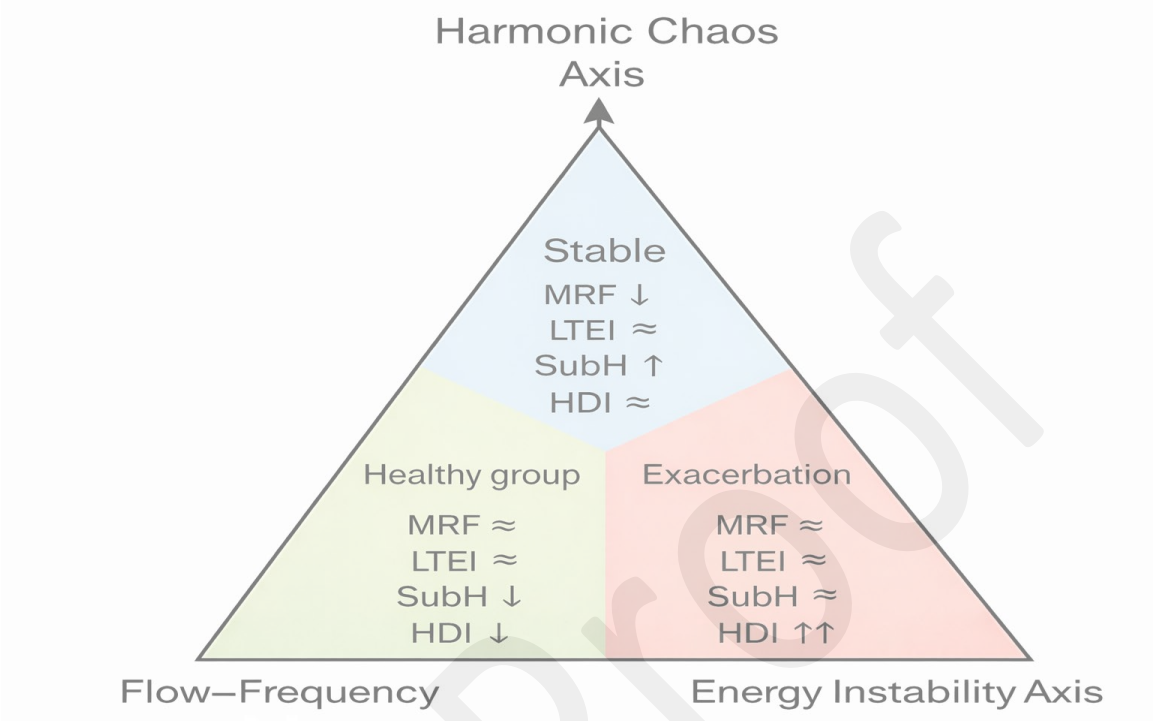

Note: The triangular schematic summarizes the directionality of each index across the three clinical states based on group medians and Holm-adjusted Dunn post-hoc comparisons following the Kruskal–Wallis test. Up/down arrows indicate relatively higher/lower values; '≈' indicates nonsignificant differences after multiplicity adjustment. MRF: Median Respiratory Frequency; LTEI: Long-Term Energy Index; SubH: Subharmonic Index; HDI: Harmonicity Deviation Index; COPD: Chronic Obstructive Pulmonary Disease. ↑: relatively higher values; ↓: relatively lower values; ≈: no significant difference after multiplicity adjustment.

Published online June 1, 2026 https://doi.org/10.15326/jcopdf.2025.0746

Online Supplement

Supplementary Table 1. Quantitative emphysema assessment on inspiratory chest CT.

	Stable COPD (n = 85)	COPD Exacerbation (n = 88)	P-value
LAA–950, % (whole lung)			
Median (IQR)	15.27 (4.81–32.99)	27.61 (14.18–35.39)	**0.002**
Mean ± SD	19.59 ± 16.21	27.33 ± 15.35	
Distribution by LAA–950 threshold, n (%)			
< 5 %	22 (25.9)	2 (2.3)	**< 0.001**
5 to < 25 %	32 (37.6)	36 (40.9)	
25 to < 50 %	26 (30.6)	44 (50.0)	
≥ 50 %	5 (5.9)	6 (6.8)	

Note: LAA–950, percentage of lung voxels with attenuation < –950 Hounsfield units; COPD, chronic obstructive pulmonary disease; IQR, interquartile range; SD, standard deviation. P-values calculated with the Mann–Whitney U test for continuous variables and Fisher's exact test for the categorical distribution.

Published online June 1, 2026 https://doi.org/10.15326/jcopdf.2025.0746

Supplementary Figure 1. Study flow diagram.

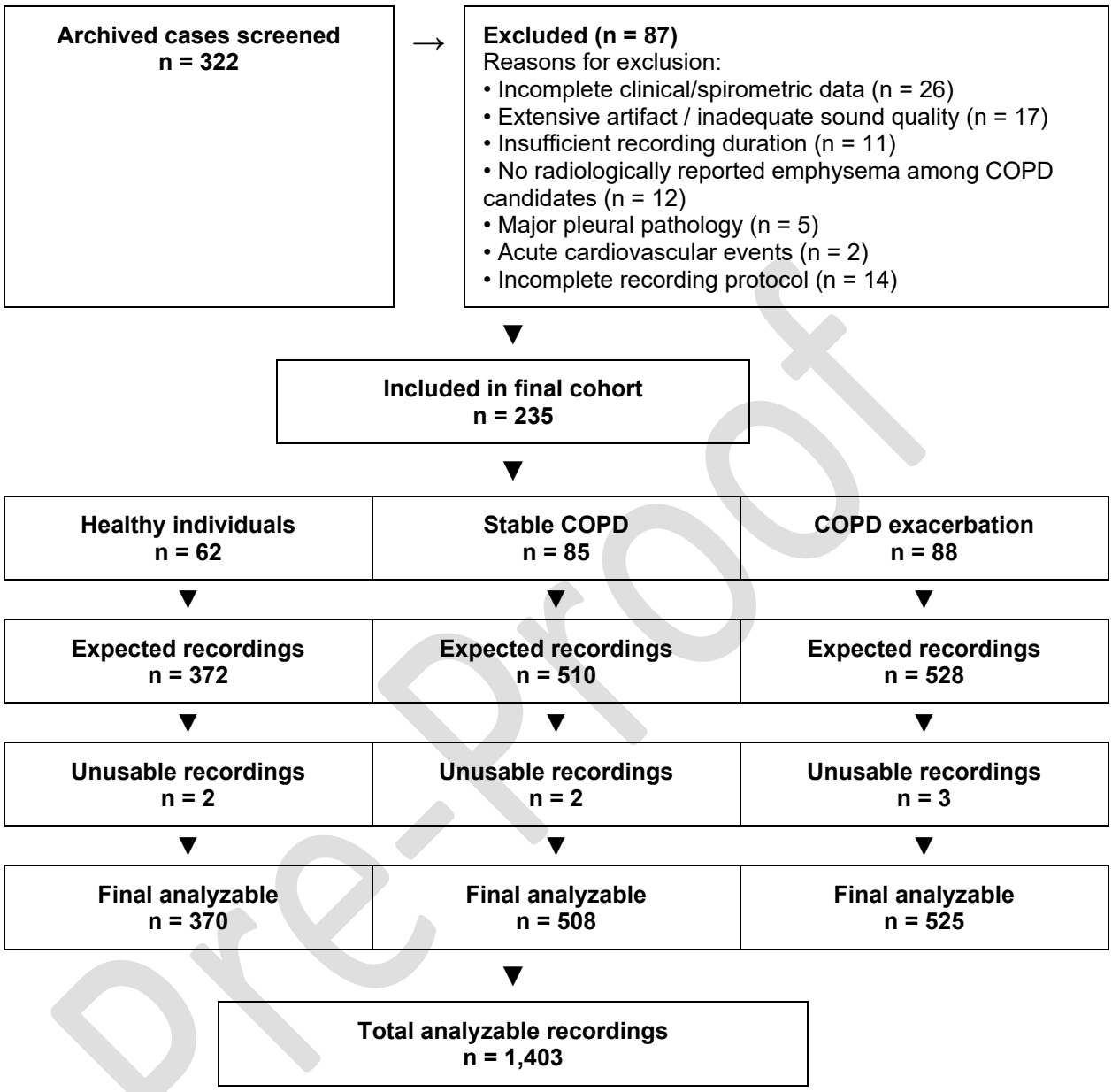

Note: A total of 322 archived cases were screened. Eighty-seven were excluded because of incomplete clinical/spirometric data (n = 26), extensive artifact or inadequate sound quality (n = 17), insufficient recording duration (n = 11), absence of radiologically reported emphysema among COPD candidates (n = 12), major pleural pathology (n = 5), acute cardiovascular events (n = 2), or incomplete recording protocol (n = 14). The final cohort included 235 participants: 62 healthy individuals, 85 patients with stable COPD, and 88 patients with COPD exacerbation. Based on the six-site posterior thoracic recording protocol, expected recordings were 372, 510, and 528, respectively. After quality control, final analyzable recordings were 370, 508, and 525, respectively, for a total of 1,403 recordings. COPD, chronic obstructive pulmonary disease.

Published online June 1, 2026 https://doi.org/10.15326/jcopdf.2025.0746

Figure S1. PCA visualization of the four-index acoustic space.

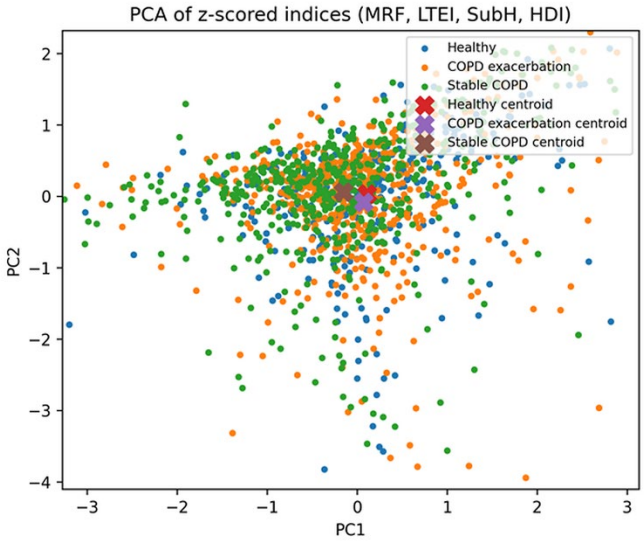

PC1-PC2 projection of z-scored MRF, LTEI, SubH, and HDI recordings, colored by clinical group; X markers indicate group centroids. Plot limits were set to improve visualization of the main cluster; 20 recordings fall outside the displayed range but are included in the PCA and all downstream analyses.

Published online June 1, 2026 https://doi.org/10.15326/jcopdf.2025.0746